Pergamon

Progress in Oceanography 43 (1999) 163–192

Progress in Oceanography

Interdecadal modulation of interannual atmospheric and oceanic variability over the North Pacific

Shoshiro Minobe[a,*], Nathan Mantua[b]

[a]*Division of Earth and Planetary Sciences, Graduate School of Science, Hokkaido University, N-10, W-8, Sapporo 060-0810, Japan*

[b]*Joint Institute for the Study of the Atmosphere and Oceans, University of Washington, Seattle, WA 98195-4235, USA*

Abstract

The interdecadal modulation of interannual variability of the atmosphere and ocean is examined over the North Pacific by using Wavelet Transform combined with Empirical Orthogonal Function (EOF) or Singular Value Decomposition (SVD) analysis. For the period of record 1899–1997, the interannual variability of the wintertime Aleutian Low, identified by either the North Pacific Index or the leading eigenvector (EOF-1) of North Pacific sea level pressure (SLP), exhibits an interdecadal modulation. Interannual variance in the strength of the Aleutian Low was relatively large from the mid-1920s to mid-1940s and in the mid-1980s, but relatively small in the periods from 1899 to the mid-1920s and from the mid-1940s to the mid-1970s. The periods of high (low) interannual variability roughly coincide with pentadecadal regimes having a time averaged relatively intense (weak) Aleutian Low. Consistent with this SLP variability the interannual variance in the zonal wind stress is strengthened in the central North Pacific after the 1970s. The SLP EOF-2, which is related to the North Pacific Oscillation, exhibited a strengthening trend from the beginning of this century to the mid-1960s. After the 1970s, the interannual variance of SLP EOF-2 is generally smaller than that in the period from 1930 to 1970. Similar interdecadal changes in interannual variance are found in expansion coefficients for the first two EOFs of the Pacific sector 500 hPa height field for the period 1946–1993. EOF-1 of Pacific sector 500 hPa corresponds to the Pacific/North American (PNA) teleconnection pattern, while EOF-2 is related to the Western Pacific (WP) pattern. The relative influence of the atmospheric PNA and WP interannual variability on North Pacific SSTs appears to have varied at pentadecadal time scales. Results from an SVD analysis of winter season (December–February) 500 hPa and North Pacific spring season (March–May) SST fields demonstrate that the PNA-related SST anomaly exhibited larger interannual variance

* Corresponding author. Fax: + 81-11-706-4907; e-mail: minobe@neptune.sci.hokudai.ac.jp

0079-6611/99/$ - see front matter
PII: S0079-6611(99)00008-7

after the 1970s, whereas the interannual variance of the WP related SST anomaly is larger before the 1970s. Correlations between the coastal North Pacific SST records and gridded atmospheric field data also change on interdecadal time scales. Our results suggest that the SST records from both the northwest and northeast Pacific coasts were more closely coupled with the PNA teleconnection pattern during the periods of 1925–1947 and 1977–1997 than in the regime from 1948 to 1976. Teleconnections between ENSO and preferred patterns of atmospheric variability over the North Pacific also appear to vary on interdecadal time scales. However, these variations do not reflect a unique regime-dependent influence. Our results indicate that ENSO is primarily related to the PNA (WP) pattern in the first (last) half of the present century. Correlation coefficients between indices for ENSO and PNA-like atmospheric variability are remarkably weak in the period from 1948 to 1976.

Contents

1. Introduction

Recent studies have revealed that decadal–interdecadal climate variations exist over the North Pacific associated with fluctuations in the strength of the wintertime Aleutian Low. The intensification of the Aleutian Low in the late-1970s has attracted much attention (e.g. Nitta & Yamada, 1989; Trenberth, 1990; Tanimoto, Iwasaka, Hanawa & Toba, 1993; Graham, 1994; Nakamura, Lin & Yamagata, 1997). This abrupt change in the mean state of the atmosphere, often termed a climatic 'regime-shift', is not unique to the late 1970s. Hare and Francis (1995), Minobe (1997) and Zhang, Wallace and Battisti (1997) showed that parallel regime shifts also occurred in the 1920s and 1940s. Mantua, Hare, Zhang, Wallace and Francis (1997) labeled this phenomenon the Pacific Decadal Oscillation (PDO) and discussed some of the impacts this mode of climate variability has on the large marine ecosystems of the North Pacific. Based upon tree-ring generated climate reconstructions, Minobe (1997) suggested that this pattern of regime-scale climate variability—or the PDO—has had a periodicity of 50–70 years over the past few centuries.

Whereas previous studies of 20th century regime shifts in the North Pacific

described the differences of the first moments—i.e. time means—between successive epochs, changes of the second moment—the variance associated with time scales shorter than those of a given regime—have not been investigated. Shorter time scale variability is of great interest as it plays an important role in the Earth's climate system and in socio-economic and ecological impacts.

The purpose of the present paper is to examine regime-scale changes in the interannual variability of the atmosphere and ocean over the North Pacific Ocean. Our work addresses the following questions: (i) Have characteristic patterns and intensities of interannual ocean–atmosphere climate variability changed on interdecadal time scales? (ii) If interannual climate variability is modulated on interdecadal time scales, are the modulations related to the interdecadal variability itself? and (iii) Do relationships between the ocean and atmosphere show evidence of change on interdecadal time scales?

2. Data and methodology

For our analysis we examine gridded SLP, 500 hPa height, wind stress and SST data sets. The monthly SLP data are updated versions of the Trenberth and Paolino (1980) archives for the period of record 1899–1997. The monthly 500 hPa height data are produced by NCAR, spanning the period of record 1946–1994. These two data sets are on a $5 \times 5°$ grid, limited to the Northern Hemisphere. The gridded zonal and meridional wind stresses and SST data are described by da Silva, Young and Levitus (1994a, b) on a $1 \times 1°$ grid for the period 1945–1993. Although the SST and wind stress data have a global coverage, we only use the data from the extratropical North Pacific (20°N to 60°N).

In addition to the gridded field data, we examine long-term coastal SST records from stations in the northeast (US/Canada) and northwest (Japan) Pacific. These stations are located between 32°N and 55°N along the Pacific coast of Canada and the United States (Fig. 1), and between 34°N and 46°N along the Pacific coast of Japan (Fig. 2). The data at La Jolla, California, begin in 1916, but the Canadian data are available only after the mid 1930s. The US and Canadian data are available through 1997. Thus, the US/Canada coastal SST data cover the time periods spanning the past 2 regimes (1948–1976, and 1977–present), with some records covering the earlier regime (1925–1947). Most of the Japanese coastal SST time series begin in the 1910s and end between 1955 and 1984. The exception is the Enoshima record, which is updated to 1995, though Enoshima SST from 1945 to 1953 was estimated from a multiple regression using neighboring stations by Kodama, Nagashima and Izumi (1995). We examine only those records that continue to at least the 1970s.

In addition to data for the North Pacific Ocean, we use the Southern Oscillation Index (SOI) and Cold Tongue Index (CTI). The SOI is defined as the sea-level pressure at Tahiti minus that at Darwin. The CTI is the average SST over 6°S–6°N, 180–90°W based on SST observations contained in COADS, produced at Joint Institute for the Study of the Atmosphere and Oceans (JISAO), University of Washington (Deser & Wallace, 1990). Although both SOI and CTI covers over the present cen-

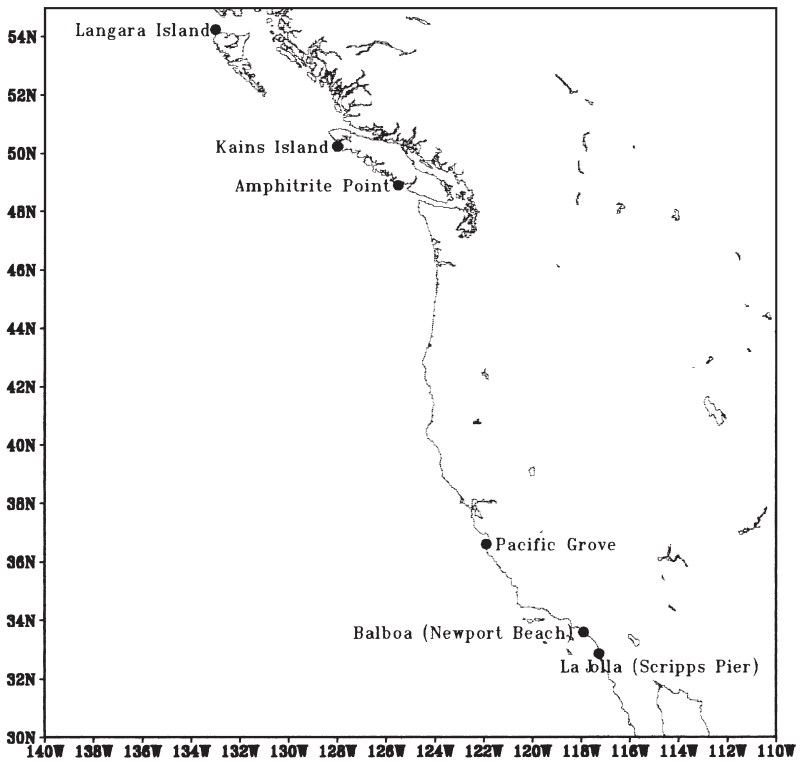

Fig. 1. Map of long-term coastal SST observing stations along west coast of United States and Canada.

tury, the Tahiti SLP used for calculating the SOI was not continuously observed in 1930s.

Gu and Philander (1995) demonstrated the utility of wavelet analysis in objectively investigating interdecadal modulations of interannual variability in the tropical Pacific. Various climate research applications of wavelet analysis can be found in Weng and Lau (1994), Lau and Weng (1995) and Torrence and Compo (1998). The essential methodology is documented in the aforementioned references. Here, we briefly summarize the main points that describe how interannual variance in a time series can be estimated using wavelet transforms.

Wavelet transform coefficients of a signal $f(t)$, which varies with time, t, are defined as follows:

$$\tilde{f}(t',a) = \frac{1}{a^{1/2}} \int f(t)\psi^*\left(\frac{t-t'}{a}\right)dt \tag{1}$$

where $\tilde{f}(t',a)$ is the wavelet coefficient, t' is the translation parameter corresponding to the position of the wavelet, a is the scale dilation parameter that determines the width of the wavelet, and ψ^* is the complex conjugate of a mother wavelet, ψ. The mother wavelet can be either a real-valued function or a complex-valued function.

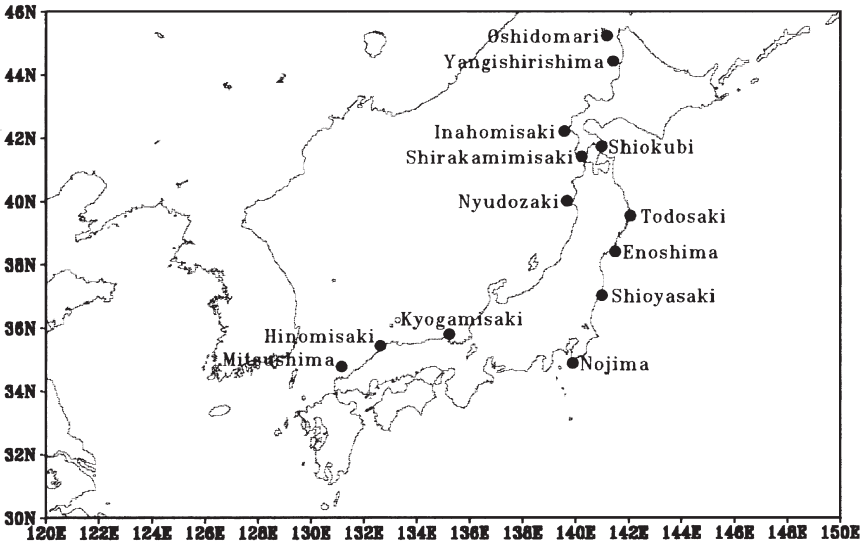

Fig. 2. Same as Fig. 1, but for the observing stations in Japan.

The complex-valued wavelet allows us to depict the amplitude (and phase) of the scale a as a function of time, and hence we can examine the interdecadal modulation of the amplitude or energy of an interannual signal (e.g. Gu & Philander, 1995). We employ the Morlet wavelet, which is a commonly used complex valued wavelet and is given by a sinusoidal function modulated by a Gaussian envelope. According to Torrence and Compo (1998), we use the mother wavelet expressed as the following form,

$$\psi(t) = \pi^{-1/4} e^{i\omega_0 t} \exp(-t^2/2), \tag{2}$$

where t has units of years, and ω_0 is a constant that defines the width of the Gaussian envelope of the mother wavelet. In the present study, ω_0 is chosen to be 6 (Farge, 1992). An important property of wavelet transforms is the conservation of energy:

$$\int_{-\infty}^{\infty} |f(t)|^2 dt = \frac{1}{C_\delta} \int_0^{\infty} \frac{da}{a^2} \int_{-\infty}^{\infty} |\tilde{f}(t',a)|^2 dt', \tag{3}$$

where C_δ is a constant and is 0.776 for the present mother wavelet (Torrence & Compo, 1998). Eq. (3) shows that the total energy can be split into different scales. The variance (E) between two scales is given by

$$E(t') = \frac{1}{C_\delta} \int_{a_1}^{a_2} |\tilde{f}(t',a)|^2 \frac{da}{a^2}. \tag{4}$$

To focus on interannual variance the scales a_1 and a_2 are chosen to correspond to periods of two and eight years, respectively. In order to avoid end effects, we extended time series by 20% at the beginning and end, using an auto-regressive model based on Maximum Entropy Method of the order of 40% of the number of observations in the available record length of each data series. In some results shown below, we use a high-pass filter, which is the fourth-order Butterworth filter. This filter is applied twice forward and backward to a time series, which results in zero phase distortion of the filtered time series. Before the filtering, the input time series is extended at its beginning and end using the Maximum Entropy Method described above.

3. Results

3.1. Large-scale atmospheric variability

The interdecadal variability and associated regime shifts have been identified in several time series used to measure the intensity of the Aleutian Low. Fig. 3(a) shows the winter North Pacific Index (NPI) defined by Trenberth and Hurrel (1994). The NPI is defined as the area-averaged SLP anomaly in the region 160°E–140°W,

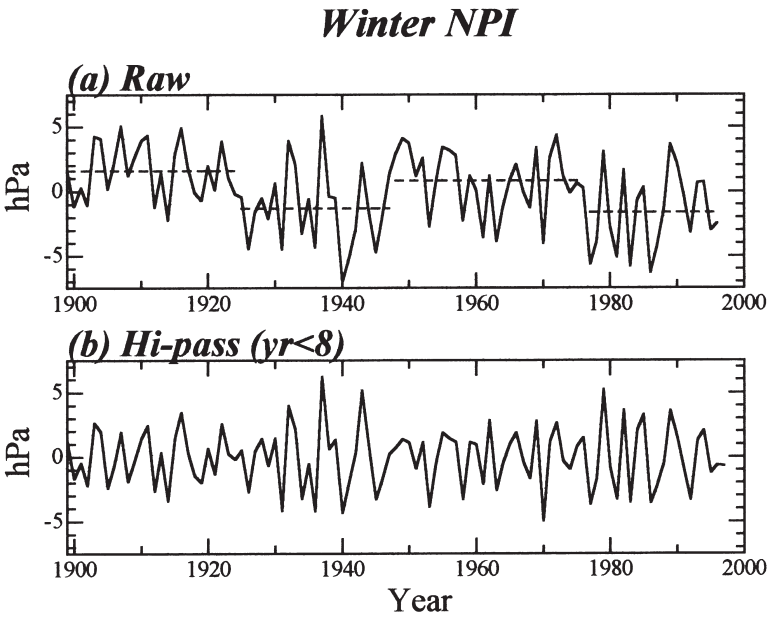

Fig. 3. Winter North Pacific Index (a) and its high-pass filtered time series with a cut-off period of eight years (b). Dashed lines in panel (a) indicate the period-means of the NPI in respective regimes from 1899–1924, 1925–1947, 1948–1976, 1977–1997.

30–65°N. This index exhibited interdecadal strengthening in the 1920s and 1970s and weakening in 1940s, marking the times of climatic regime shifts (Hare & Francis, 1995; Mantua et al., 1997; Minobe, 1997). An analysis of the winter–spring NPI identifies peak spectral power at periods of about 50 years (Minobe, 1997), and also time frequency structure obtained by the wavelet supports the timescale from 50 to 60 years (Minobe, 1999). This estimate is approximately consistent with the fact that 20th century regimes have persisted from 20 to 30 years. In the present paper, we refer the oscillation associated with the repeating regime shifts as *pentadecadal variability*.

From a visual inspection of the NPI, an interesting feature is the suggestion that the amplitude of interannual NPI variability does not appear to be constant in time. The appearance of an interdecadal modulation of interannual variability becomes more prominent when we apply a high-pass filter to the time series (Fig. 3(b)).

In order to describe quantitatively the interdecadal modulation of the interannual variability of the winter (December–February) NPI, we calculated the interannual variance as a function of time using wavelet coefficients as defined in Eq. (4) (Fig. 4). The time history of the NPI variance supports the aforementioned visual inspection of Fig. 3. The variance from 1930 to 1945 and in the 1980s is about 2 or 3 times as large as the variance for other periods. It is noteworthy that these local maxima of interannual variance are found in the regimes identified as having an especially intense (mean-state) Aleutian Low. The present result is consistent with Hanawa (1997), who showed that NPI differences between two successive years is large (small) in the regimes with the strong (weak) Aleutian Low. In summary, energetic

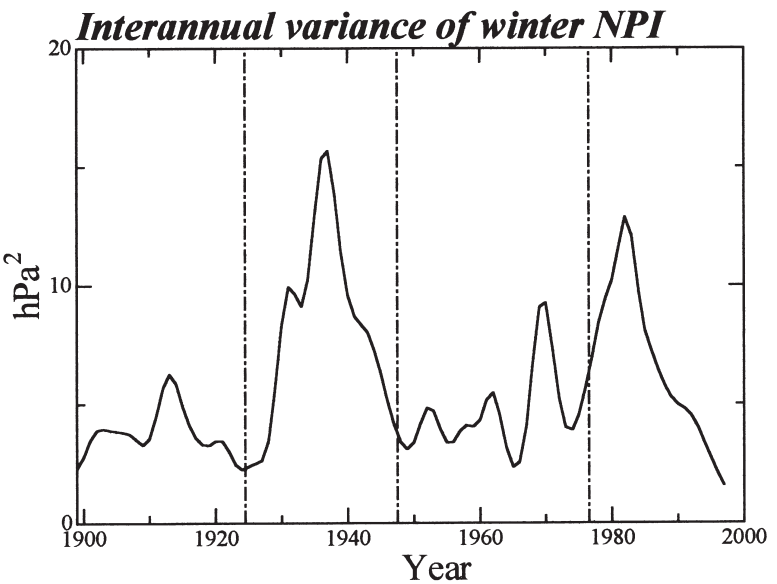

Fig. 4. Interannual (2 yr < periods < 8 yr) variance of winter NPI. Dot-dashed lines indicate the time of regime shifts at 1924/25, 1947/48, 1976/77.

(relatively weak) interannual variability of the Aleutian Low was observed in the intense (relatively weak) Aleutian Low regimes associated with the pentadecadal oscillation. Consequently, the severe winter in the regime with the intense Aleutian Low tends to be more severe than that expected from the regime-mean difference resulting from the enhanced interannual variances, whereas difference in the Aleutian Low strength for moderate winter tends to be smaller than the regime-mean difference. Therefore, the differences between regimes are prominent in severe winters in respective regimes than moderate winters.

The significance of the changes of interannual variance of the high-pass filtered NPI shown in Fig. 3(b) is examined by a f-test, assuming the data in each year are independent. The changes in interannual variance associated with the regime shifts are significant at 95% confidence level for the shifts in the 1920s and 1940s, though the change for the last shift in the 1970s is only significant at 85% confidence level. In the last regime, the large interannual variance is confined in the 1980s and not seen in the 1990s. In the case where we examine the interannual variance change between two periods from 1948 to 1976 and from 1977 to 1989, the change is significant at 95% confidence limit. We assume that the present regime is not yet over, hence we need future data in order to conclude whether the variance changes are significant for the two periods determined by regime shifts for the before and after the regime shift in the 1970s.

We also examine EOF modes for the winter SLP over the North Pacific (120°E–90°W, 20–70°N) (Fig. 5). The first EOF exhibits the SLP changes associated with the Aleutian Low variability, while the second EOF captures variability associated with the North Pacific Oscillation (NPO; Walker & Bliss, 1932; Rogers, 1981). Note that the NPO is linked with the Western Pacific teleconnection pattern aloft (Wallace & Gutzler, 1981). The first and second modes explain 43.6% and 17.3% of the total variance, respectively. The temporal coefficient of the first EOF is nearly identical to that of the NPI, with the correlation coefficient between them being 0.98. Thus, the interdecadal modulation of interannual variability shown in the NPI is repeated by the expansion coefficient for the first EOF mode (Fig. 6). The interannual variance of the expansion coefficient for the second EOF mode exhibits an increasing trend from the beginning of the present century to the mid-1960s, with a 10–20 year period fluctuation. After 1970, the interannual variance of the second mode is smaller than that from 1930 to 1970.

We calculated the EOFs for the high-pass filtered North Pacific (120°E–80°W, 20–70°N) SLP in respective regimes. The spatial structures of the first and second EOF modes are unchanged from one regime to the next. In all regimes, the first mode is related with variations in the intensity of the Aleutian Low, and the second mode is associated with the North Pacific Oscillation. The absolute and relative (to the total field) variance contributed by the first mode, however, is regime-dependent. The variance resulting from the first mode is 1.6–2.1 times larger in the strong Aleutian Low regimes (periods of 1925–1947 and 1977–1997) relative to that in the weak Aleutian Low regimes (periods of 1899–1924 and 1948–1976). The variance explained by the first EOF mode reached 51–54% for the periods of 1925–1947 and 1977–1997, but was only 35–38% in 1899–1924 and 1948–1976.

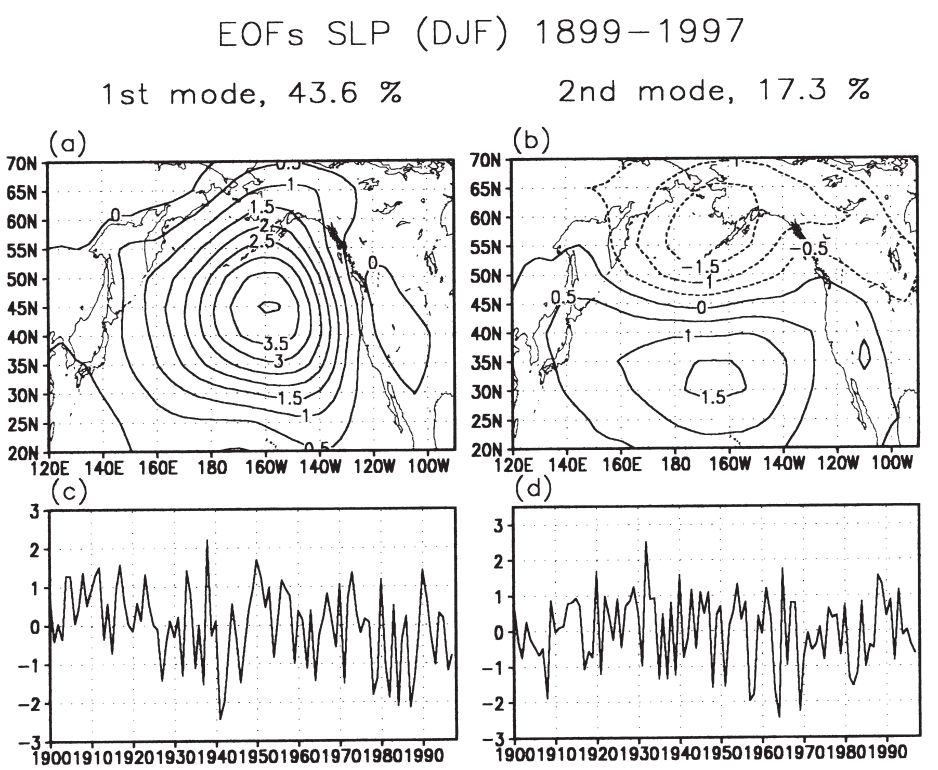

Fig. 5. Spatial patterns of the first (a) and second (b) EOF modes and their temporal coefficients (c and d) for the SLP in winter season (December–February) over the North Pacific (120°E–90°W).

The spatial distribution of the interdecadal changes in interannual variability can be examined by comparing the variance of high-pass filtered winter SLP at each grid point in different epochs (Fig. 7). The variance from 1925 to 1947 and from 1977 to 1997 is large in the North Pacific. The spatial patterns indicate that the variance maxima are capturing energetic interannual variations in the intensity of the Aleutian Low. Additional notable features include the variance changes in the Arctic region. In the period after the mid-1970s, variance in this region is large while in the period from 1948 to 1976 the variance is relatively small. From 1925 to 1947, although the sampling over the Arctic is poor, the local maximum at 60°E 70°N suggests that the interannual variance over the Arctic was also large in this period. Similar but minor interdecadal changes appear west of England. Although we limit our detailed investigations to the North Pacific sector, the present results suggest that interdecadal modulations of the interannual variability have hemispheric distributions that are especially related with the Arctic.

Aleutian Low variability, as represented by either the NPI or the expansion coefficient for the leading EOF of North Pacific SLP, is known to be highly correlated with variability in the Pacific/North America (PNA) teleconnection pattern

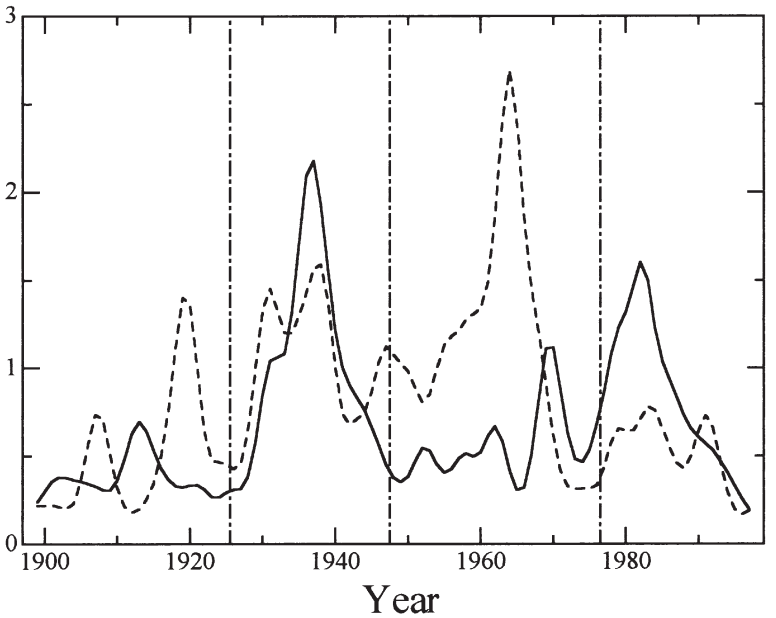

Fig. 6. Same as Fig. 4, but for the EOF-1 (solid curve) and EOF-2 (dashed curve) of winter SLP over the North Pacific shown in Fig. 5.

(Trenberth & Hurrel, 1994). Thus, it is interesting to examine whether the interdecadal modulation of the interannual variability found in the NPI is also seen in the PNA pattern. Fig. 8 shows the spatial patterns of the first and second EOF modes and their temporal coefficients for the 500 hPa height in winter season (December–February) over the North Pacific (120°E–90°W, 20–80°N). The first mode is similar to the PNA pattern, while the second mode resembles the Western Pacific (WP) teleconnection pattern. The correlation coefficient between expansion coefficients for the first (second) EOF mode of the 500 hPa height and that of the first (second) EOF mode of the SLP is 0.95 (0.80). Wallace and Gutzler (1981) have noted the strong coherence between the WP and North Pacific Oscillation patterns. Interdecadal modulations of the interannual variability of the first and second modes of 500 hPa height fields are similar to those of the first two modes of SLP (Fig. 9, compare with Fig. 6), suggesting that the pentadecadal oscillation modulates the interannual variability associated with the PNA pattern. Although the interannual variability of the WP pattern exhibits significant weakening in the 1970s, it is not clear whether this change has a significant relationship with the regime shift in the 1970s. As noted previously, the interannual variability of SLP-EOF2 does not have a unique relationship with the regime shifts.

We also examined regime dependent map of the interannual variability in Northern Hemisphere 500 hPa height field for two periods from 1948 to 1976 and from 1977 to 1994. The changes of the interannual variance of the 500 hPa height variance is quite similar to the changes of the interannual SLP variance shown in Fig. 7, and

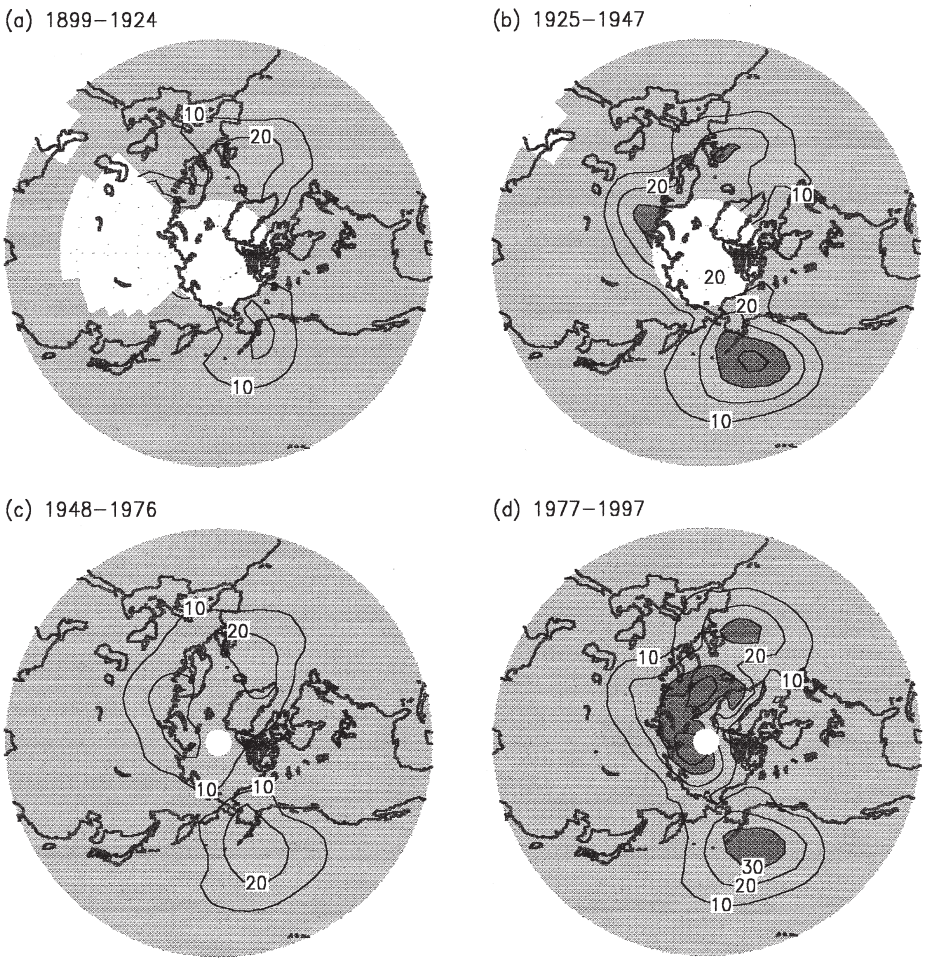

Fig. 7. Variance of high-pass filtered (yr $<$ 8) SLP in each period of 1899–1924, 1925–1947, 1948–1976, and 1977–1997. Contour interval is 10 hPa^2. Dense shading indicates gridpoints where the absolute value of the variance is larger than 30 hPa^2, while weak shading indicates where the variance is calculated (no shading indicate variance is not calculated).

hence are not shown in the present paper. The interannual variance of the 500 hPa height is characterized by the stronger variance in the latter period over the North Pacific along with increased variances over the Arctic Sea and northern North Atlantic Ocean.

Regime dependent changes of the interannual variability in North Pacific surface wind stress fields are shown in Fig. 10. Following the 1977 regime shift zonal wind stress variance in the central North Pacific is enhanced, consistent with the strengthening of the interannual variability in the SLP and 500 hPa fields. The centers of the strong variability for both the zonal and meridional wind stress in the Bering

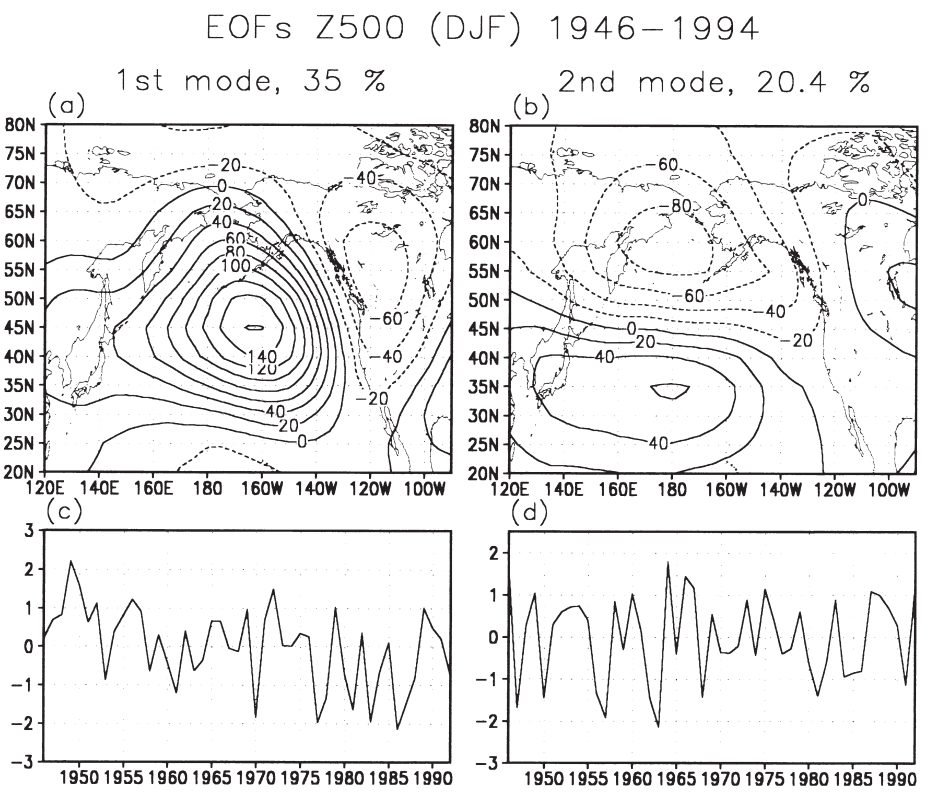

Fig. 8. Spatial patterns of the first and second EOF modes of winter (December–February) 500 hPa height (a and b) and time series of expansion coefficient of these two modes (c and d).

and Okhotsk Seas in the former period are not observed in the latter period. In the latter period, the center of the strong variability in the zonal wind stress is located near the Kamchatka peninsula. The changes of the interannual variability of the wind stresses, which force the ocean dynamically and thermodynamically through wind speed dependent heat and momentum fluxes are expected to cause changes in the interannual variance in the North Pacific Ocean.

3.2. SVD analysis of North Pacific SST and atmospheric 500 hPa fields

Interdecadal changes in the (atmospheric) SLP and 500 hPa height interannual variability suggest that linkages between the atmosphere and ocean might also vary on interdecadal time scales. In order to examine the basin scale interdecadal modulation of the atmosphere–ocean interaction on interannual time scales we performed singular value decomposition (SVD) analysis between 500 hPa height and SST fields. The 500 hPa field is examined because this field is suitable for looking at the atmospheric teleconnection patterns, and linkages between the atmosphere and ocean are

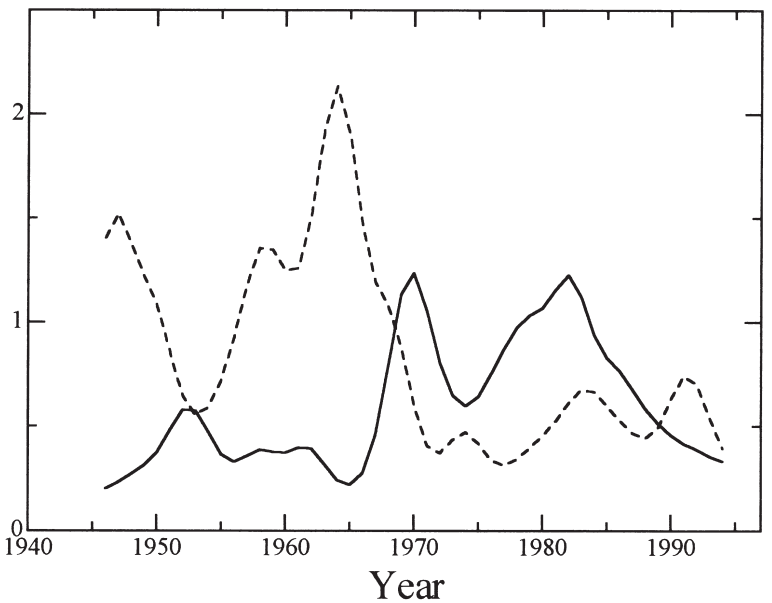

Fig. 9. Same as Fig. 4, but for the first (solid) and second (dashed) EOF time series shown in Fig. 8(c and d), respectively.

often discussed in terms of those teleconnection patterns (e.g. Wallace, Smith & Bretherton, 1992). The oceanic variability forced by the atmosphere does not need to have an amplitude maximum in the winter season, as the oceanic variability might lag the atmospheric forcing by as much as a few months. In fact, recent work suggests that the strongest relationship between the atmosphere and ocean in the mid-latitudes is realized when the variability of the ocean lags that in the atmosphere by two or three months (i.e. Koide & Kodera, 1997). For our SVD analysis, we examine the covariance between wintertime (December–February) 500 hPa height and springtime (March–May) SST fields.

The atmospheric and oceanic spatial patterns produced by our SVD analysis are essentially the same as those obtained by Wallace et al. (1992). The first mode of the atmospheric circulation exhibits a pattern similar to the PNA pattern, accompanied by a SST anomaly in the central North Pacific with an anomaly of opposite polarity along the Pacific coast of North America (Fig. 11). The second mode of the 500 hPa resembles the WP pattern, with meridional seesaw pattern of the SST in the western North Pacific. The temporal coefficients of the first and second mode of the 500 hPa height are similar to those obtained via EOF analysis (shown in Fig. 8). Likewise, the temporal coefficients for the first and second mode of SST are well correlated with the corresponding time coefficients of 500 hPa height.

Changes in the interannual variance in the temporal coefficients of the SVD modes, calculated with wavelet transforms, are shown in Fig. 12. The interannual spring SST variability related with the winter PNA pattern exhibits strong interannual varia-

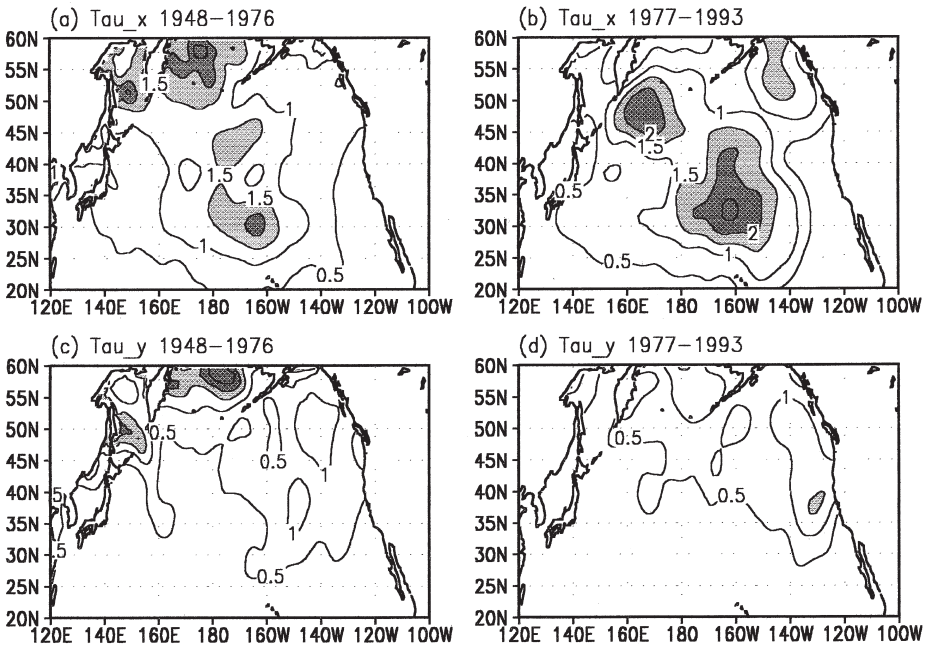

Fig. 10. Same as Fig. 7, but for the winter (December–February) zonal wind stress (a) and meridional wind stress (b) in each period of 1948–1976, and 1977–1993. Contour interval is 10^{-3} Nm^{-2}, and the numbers for the contour label are multiplied by 1000. Dense (weak) shading indicates gridpoints where the absolute value of the variance is larger than 1.5×10^{-3} (1.0×10^{-3}) Nm^{-2}.

bility after the 1970s (relative to the few decades prior), whereas the SST variability associated with the WP pattern is larger before the 1970s. Interdecadal changes in the interannual variance of the wintertime atmospheric circulation appear to be causing the parallel changes in springtime SST variability. In other words, the influence of interannual variability of the wintertime atmospheric circulation is more prominent in the springtime SST after the 1970s. This is consistent with the increasing trend of the SST persistency documented by Namias, Yuan and Cayan (1988) for the data from 1950 to 1984.

3.3. Coastal SST relationships with large-scale atmospheric circulation

For an assessment of the interdecadal modulation of the atmosphere–ocean interactions, it is desirable to use oceanic time series with the longest time history available. The SST data produced by da Silva et al. (1994b) is available after 1945, and therefore to examine the modulation of the atmosphere–ocean interactions prior to the 1940s we must use another data set. Although some gridded SST data, i.e. *Global Ocean Surface Temperature Atlas* (GOSTA) (Bottomley, Folland, Hsiung, Newell & Parker, 1990), are available for the early 20th century, sampling rates were especially poor in the ocean interior prior to World War II. Furthermore, large changes in

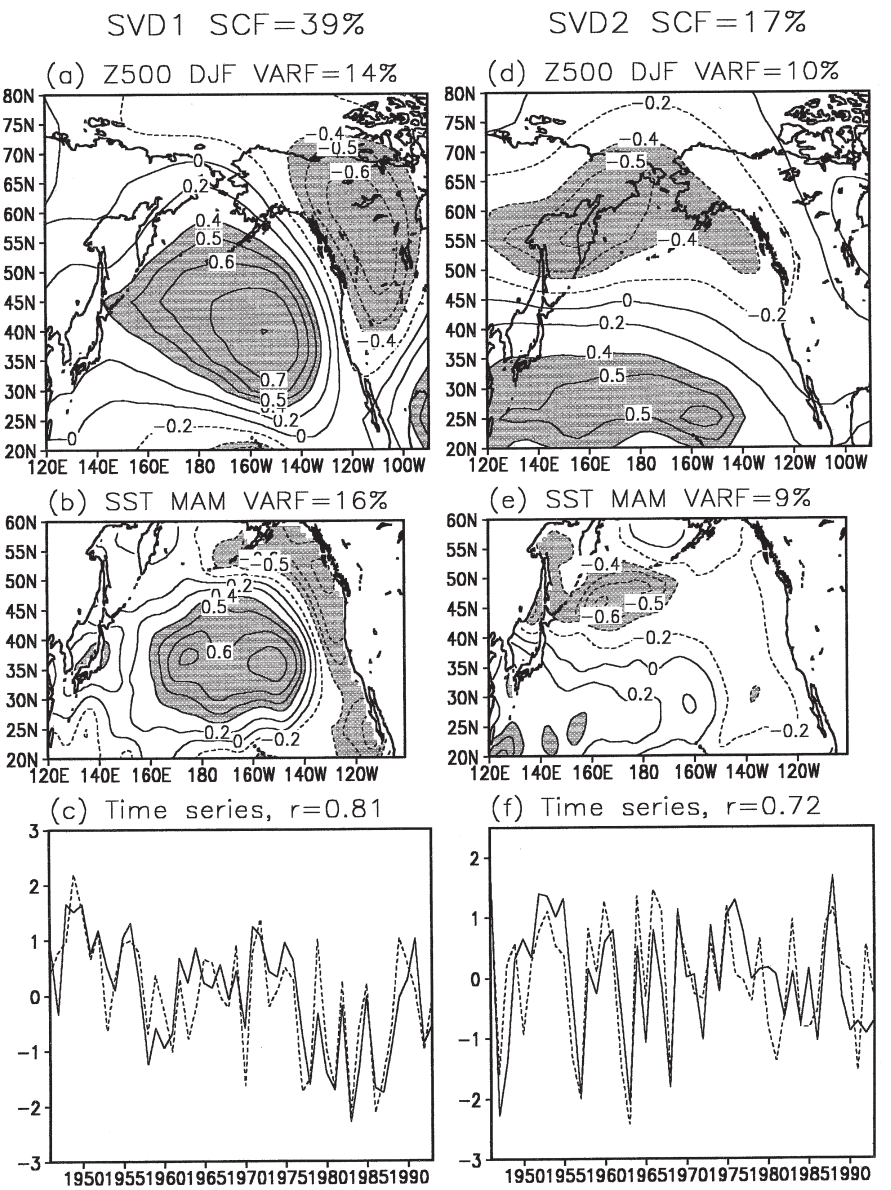

Fig. 11. The first (left panels) and second (right panels) SVD mode of winter (December–February) 500 hPa height and spring (March–May) SST over North Pacific for 1946–1993. (a and d) Heterogeneous correlation map for 500 hPa height. (b and e) Heterogeneous correlation map for SST. Contour intervals of correlation maps are 0.2 where the absolute correlation coefficient is smaller than 0.4 and 0.1 otherwise. Shading indicates grid points where the absolute heterogeneous correlation is greater than 0.4. (c and f) Time series of the normalized expansion coefficients for 500 hPa height (dashed curve) and SST (solid curve).

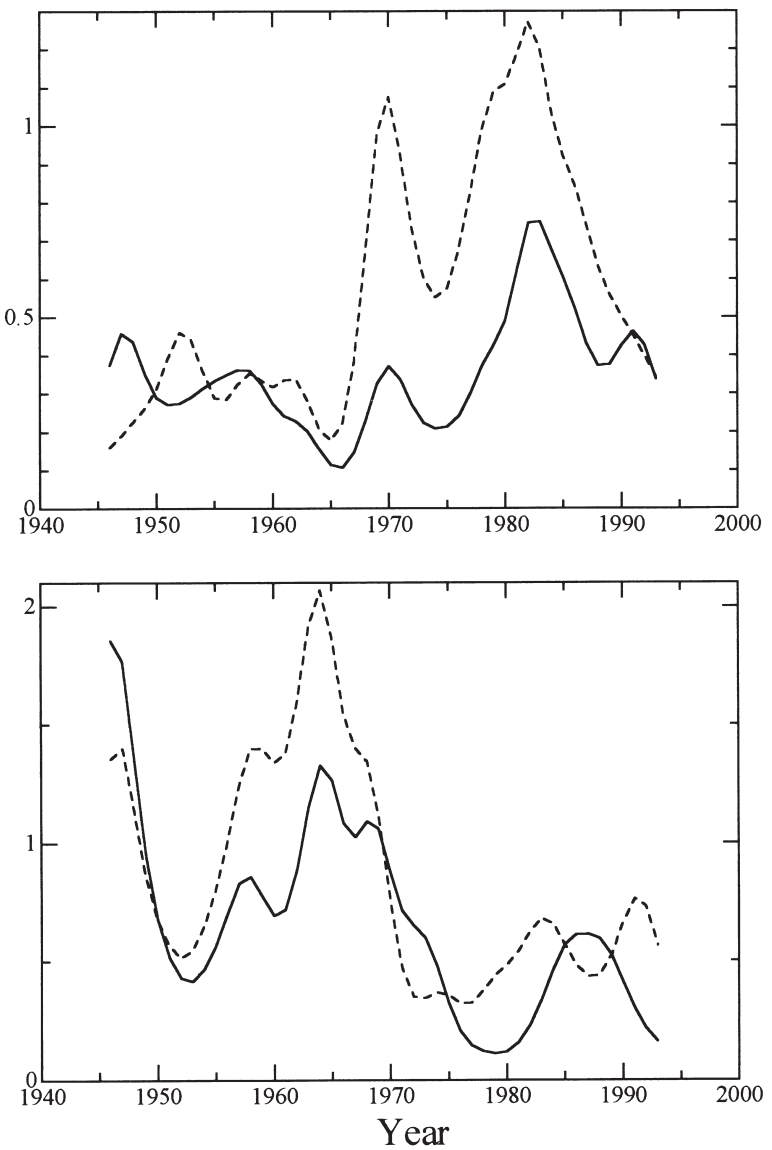

Fig. 12. Interannual variance of time series of SVD-1 (upper panel) and SVD-2 (lower panel) shown in Fig. 11(c and f), respectively. The solid (dashed) curve indicates the variance for SST (500 hPa height) time series.

sampling rates might introduce spurious changes in our estimates of time varying interannual variability. Therefore, we examine long-term coastal SST data, which are much less affected by data collection problems.

As a first step, we conduct a seasonally combined EOF analysis for the US/Canada

coastal SST data between 1935 and 1997. For this analysis, we compute EOFs from a covariance matrix constructed from the yearly time series for each season at each station. The resulting principal components thus provide information on the year-to-year variability in each season.

The eigenvector for the 1st principal mode explains 44.8% of the total variance and is characterized by springtime (March–May) maxima at all stations (Fig. 13(a and b)). The wintertime amplitude is also strong in the US stations. The expansion coefficient for the leading EOF of US/Canada coastal SST is shown in Fig. 13(c).

Maps of the correlation coefficients between the high-pass filtered March–May leading principal component of the coastal US/Canada SST and 500 hPa heights reveal an apparently consistent relationship with the PNA teleconnection pattern in the 1977–1994 regime (Fig. 14(a)). (High-pass filtering prior to calculating the correlation coefficients is used in order to avoid the influence of the decadal-to-interdecadal variability on the correlation maps.) On the other hand, this relationship is not well reproduced by the correlations for the 1948–1976 regime (Fig. 14(b)). In the 1948–1976 regime, the wavelike pattern of correlation centers is still observed. However, the latitudes of the peak correlation centers in the northern North Pacific and northern North America are shifted about 10 degrees southward and amplitudes are smaller than those in the 1977–1994 regime.

We then calculated regime dependent correlations between the high-pass filtered winter La Jolla SST and the winter SLP field (Fig. 15). A well-developed pattern of negative SLP anomalies correlated with the coastal SST data is observed in the regimes from 1925 to 1947 and from 1977 to 1997. On the other hand, the correlation coefficients are much weaker in the regime from 1948 to 1976. This regime-dependent relationship between the SLP and La Jolla SST is consistent with the regime dependent relation between the principal component of coastal SST EOF-1 and 500 hPa height. Both results indicate that the PNA pattern and strength of the Aleutian Low is more tightly coupled to the US/Canada coastal SST during the regimes with the stronger Aleutian Low, relative to the coupling during the regime with the weaker Aleutian Low.

The same analysis was carried out with the coastal Japanese SST records and gridded atmospheric data. We calculated the seasonally combined EOF of the Japanese SST data from 1915 to 1980.

The eigenvector for the first principal mode explains 26.9% of the total variance. Notice that the variance explained by the first mode is much smaller than that for the US/Canadian coastal SSTs. The first mode has an amplitude maximum at the Enoshima station in the spring season (Fig. 16(a)). The correlation coefficient between the expansion coefficient (principal component) for the first EOF and spring Enoshima SST is 0.91 (Fig. 16(b)). Therefore, we can assume that the principal component for this mode can be approximated by the springtime Enoshima SST. This assumption allows us to examine the atmosphere–ocean interaction for more than 80 years. It should be noted that the Enoshima SST is known to be a good proxy of the anomalous southward intrusion of Oyashio along the Pacific coast of Japan (Kodama et al., 1995). Sekine (1988) suggested that the anomalous southward Oyashio intrusion is caused by wind-forcing anomalies over the North Pacific, and

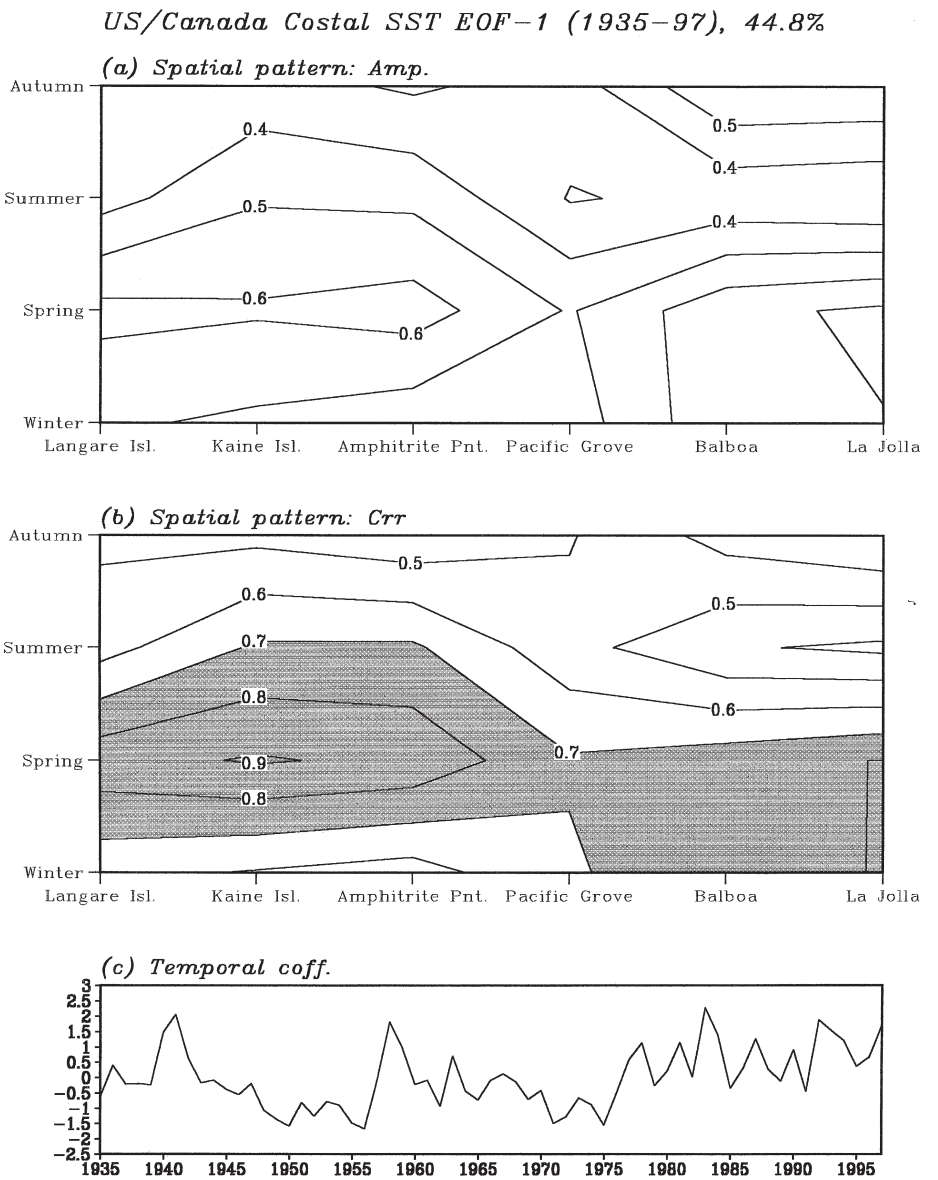

Fig. 13. Eigenvector (a), correlation pattern (b) and temporal coefficient (c) of the first seasonally combined EOF mode of coastal SST data in Unites States and Canada.

Minobe (1997) showed that the three regime shifts in the 1920s, 1940s and 1970s are detectable in the Enoshima SST.

A pair of maps depicting the correlation coefficients between springtime (March–May) Enoshima SST and wintertime (December–February) 500 hPa height for the

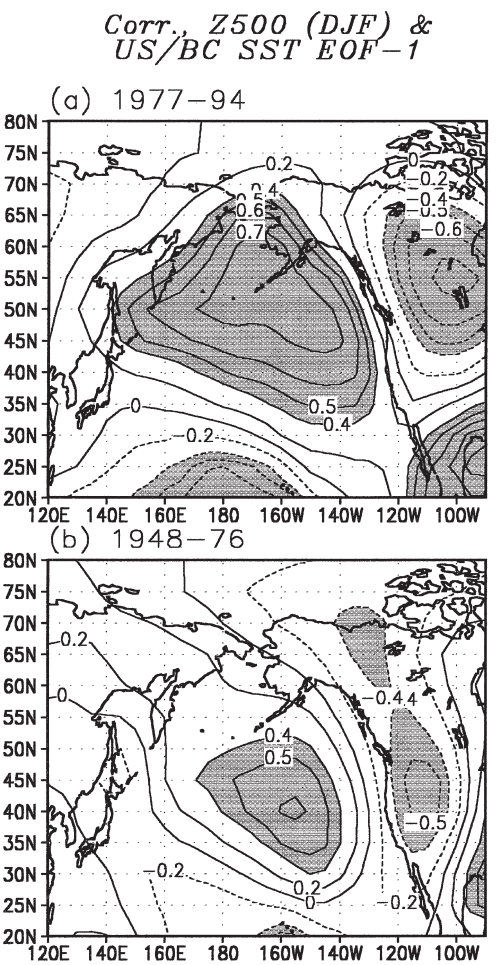

Fig. 14. Regime dependent correlation maps of the high-pass filtered winter 500 hPa height and the temporal function of seasonally combined EOF-1 of coastal SST in United States and Canada in the period 1977–1994 (a) and 1948–1976 (b).

periods 1977–1994 and 1948–1976, respectively, suggest that the atmospheric coupling to coastal SST in the northwest Pacific has also varied on interdecadal time scales (Fig. 17). In each period, the maximum correlation coefficients are located over Japan, and somewhat resemble the WP pattern. For the period of 1977–1994, the anomaly over western northern North America suggests that variability in the PNA pattern also contributes to that in Enoshima SST. However, this feature is much less apparent for the period of 1948–1976.

Maps showing correlation coefficients between springtime Enoshima SST and wintertime SLP also capture regime-related changes in coastal Japan SST relationships with the atmospheric circulation (Fig. 18). For the 1977–1997 (Fig. 18(a)) and

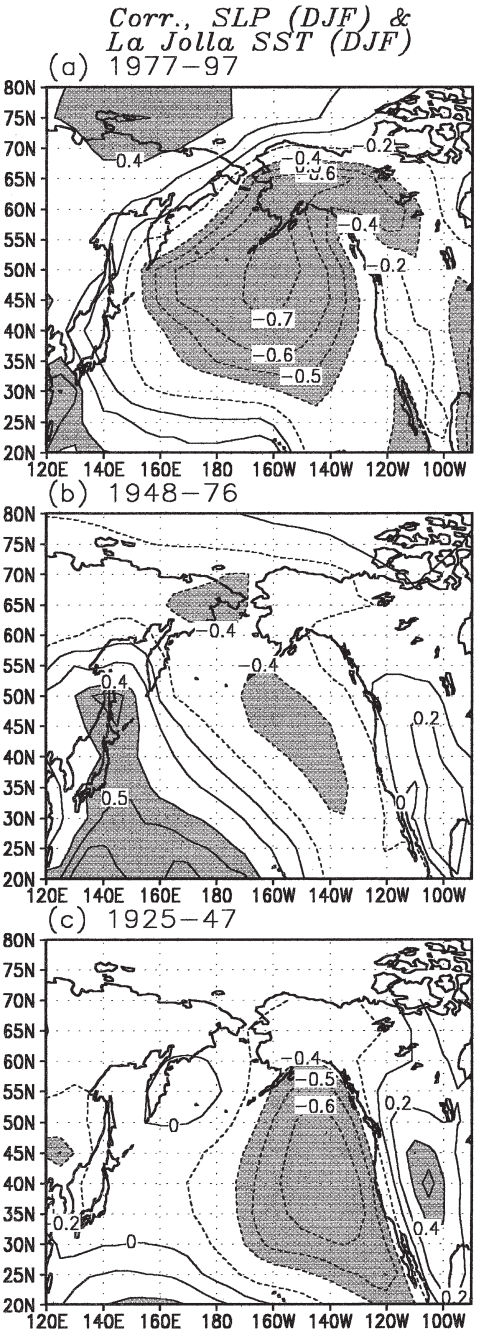

Fig. 15. Same as Fig. 14, but for the high-pass filtered winter SLP and winter La Jolla SST in the period 1977–1997 (a), 1948–1976 (b), and 1925–1947 (c).

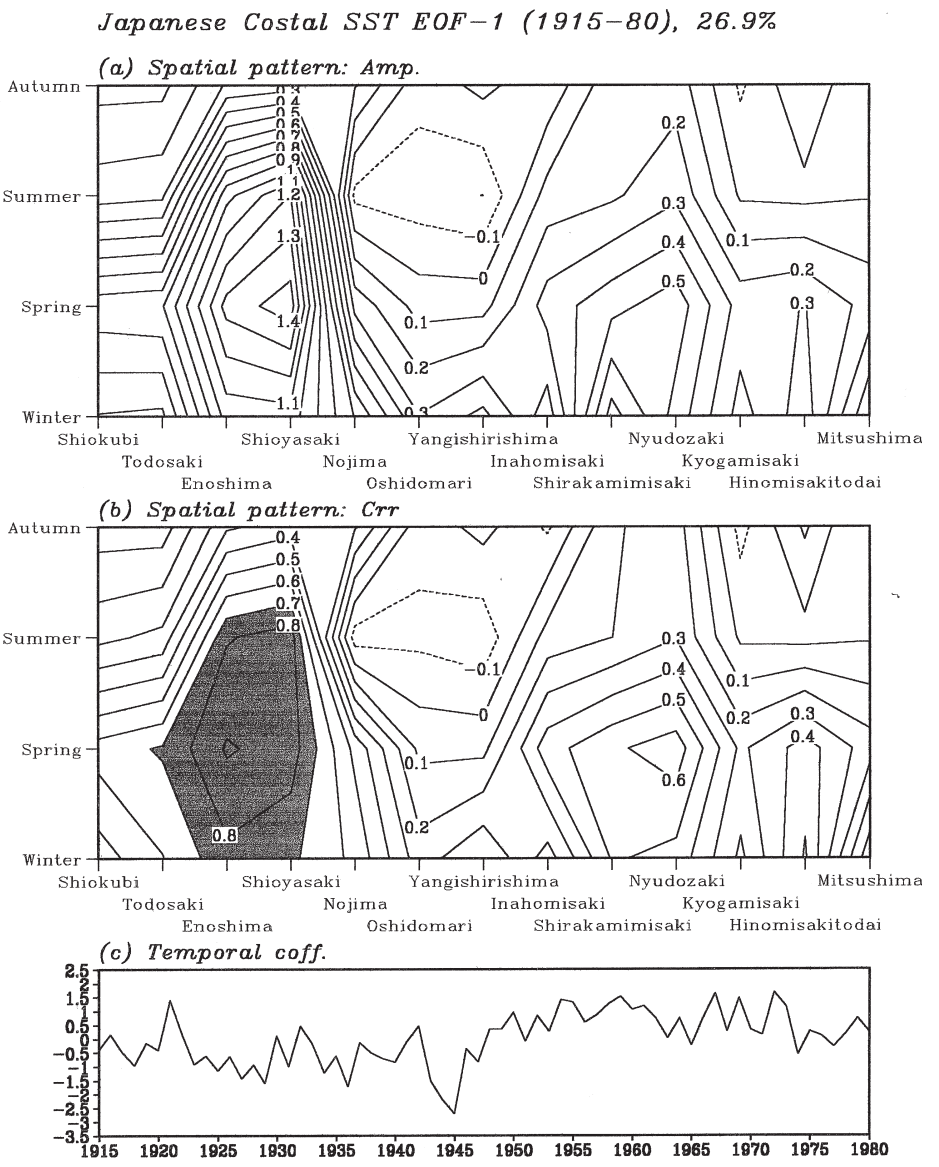

Fig. 16. Same as Fig. 13, but for the coastal SST in Japan.

1925–1946 periods (Fig. 18(c)), large-scale negative correlations over western North America again suggest coherence with the PNA pattern. On the other hand, this pattern is absent for the 1948–1976 period (Fig. 18(b)).

Recently, McGowan, Cayan and Dorman (1998) showed that the coastal SST data at La Jolla is well correlated with basin scale wintertime SST variations in the north-

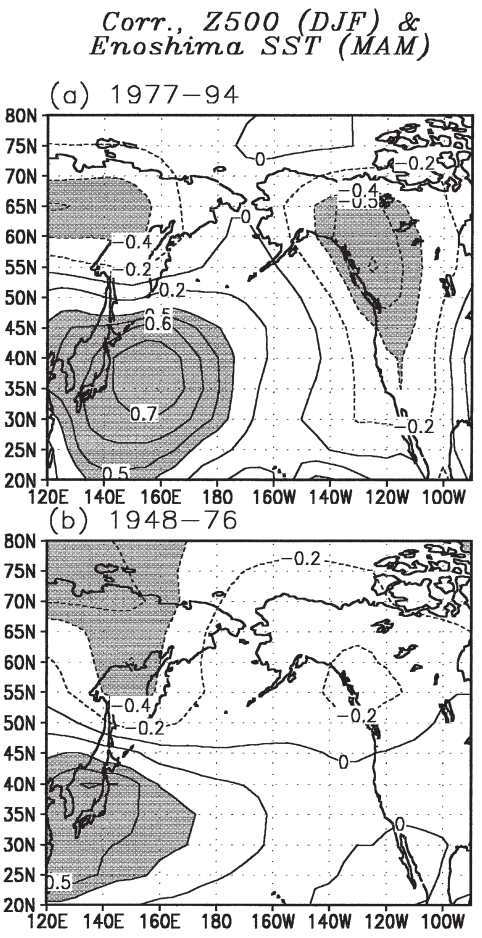

Fig. 17. Same as Fig. 14, but for the high-pass filtered winter 500 hPa height and spring Enoshima SST.

ern North Pacific (reproduced in Fig. 19(a)). We examined whether a similar basin-scale relationship is found with springtime Enoshima SST. The correlation coefficients between the wintertime North Pacific gridded SST and springtime Enoshima SST are generally weak through the 1945–1993 period or record (Fig. 19(b)). However, if we examine the regime dependent correlation coefficients between the coastal SST and gridded SST data, Enoshima SST is generally best correlated with North Pacific SSTs from 1977 to 1993 (Fig. 19(c and d)), while the La Jolla SST is best correlated with North Pacific SSTs in the period from 1948 to 1976 (Fig. 19(e and f)).

If we high-pass filter the data prior to the correlation calculations, the amplitude of the correlation coefficients after 1977 is equivalent for the La Jolla and Enoshima stations (not shown). This suggests that springtime Enoshima SST provide secondary but useful information in order to know the state of the winter SST variability in

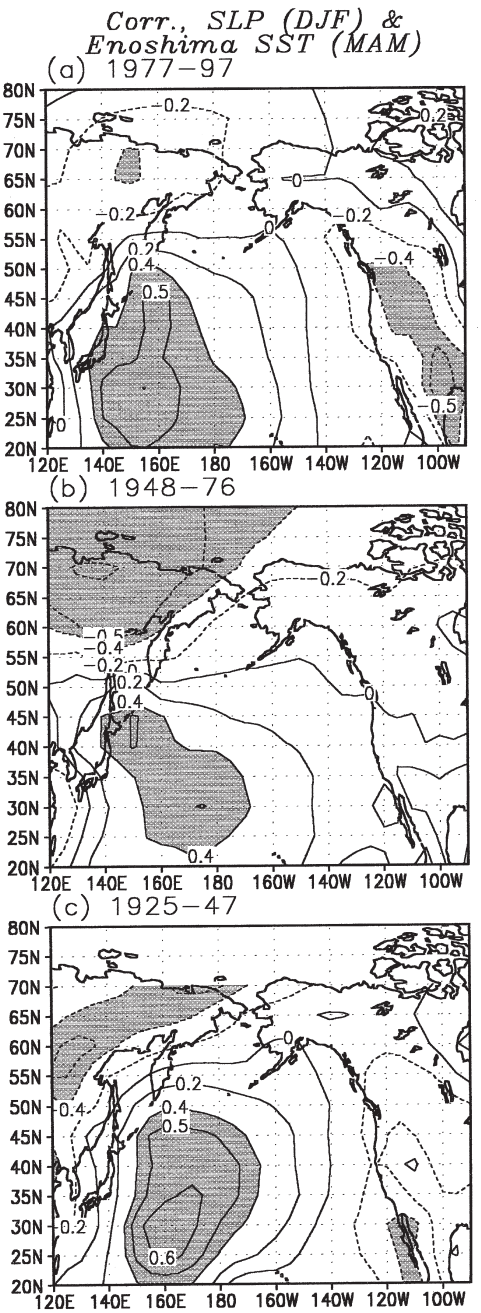

Fig. 18. Same as Fig. 15, but for the high-pass filtered winter SLP and spring Enoshima SST in the period 1977–1994 (a), 1948–1976 (b), and 1925–1947 (c).

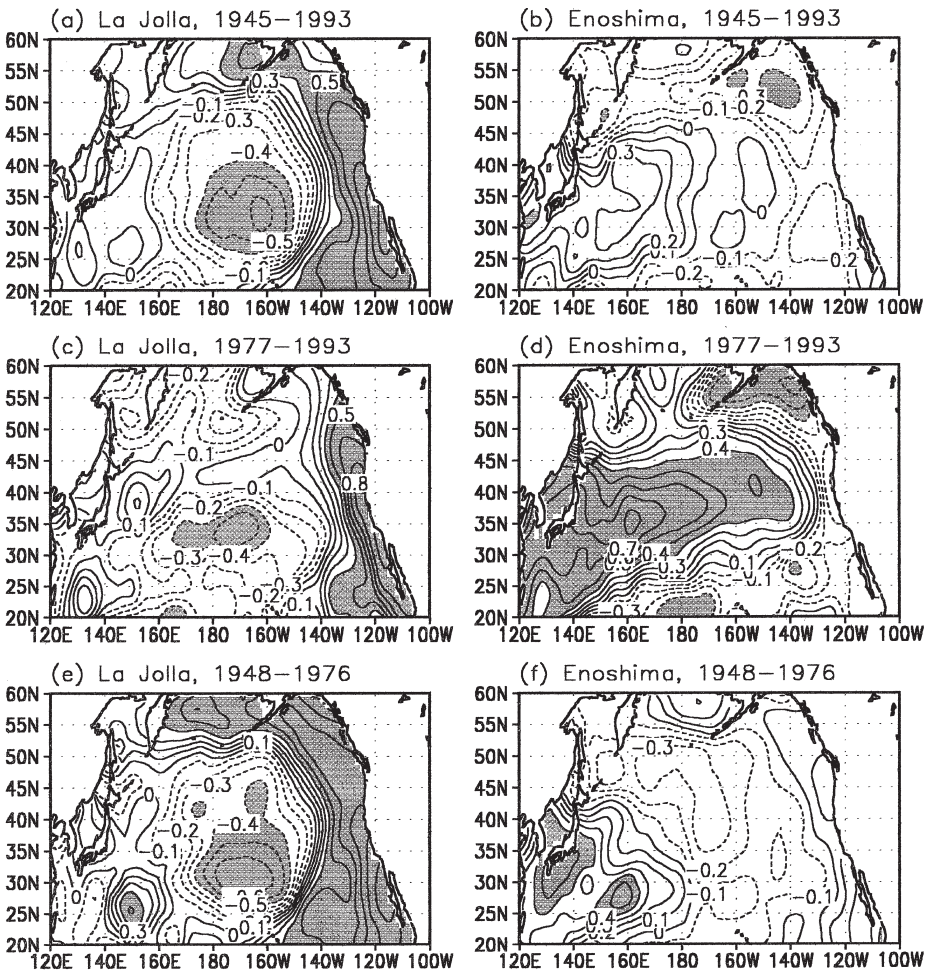

Fig. 19. Correlation maps of the winter gridded SST and the winter La Jolla SST (a, c and e) and maps of the winter gridded SST and the spring Enoshima SST (b, d and f) in the period 1945–1994 (a and b), 1977–1993 (c and d) and 1948–1976 (e and f).

the central North Pacific along with the primary information provided US/Canadian coastal SST data.

3.4. Relation between the mid-latitude and tropics

In order to examine relationships between tropical variability and midlatitude interdecadal modulations of interannual variability we calculated high-pass filtered regime dependent correlation coefficients between indices for El Nino and Southern Oscillation (ENSO) and principal components for North Pacific atmospheric circulation.

Table 1 shows a weak interannual ENSO–PNA correlation in the 1948–1976 period compared with that after 1977. The correlation coefficients between the SOI and first principal component of the SLP are larger than those between the SOI and the second principal component in the first two regimes in the present century, while the opposite is found in the latter two regimes. The first and second principal components are related with the PNA and WP patterns aloft, respectively, as noted earlier. Therefore, the correlation change between the SOI and the first two principal components suggests that ENSO was primarily correlated with the PNA pattern in the first half of this century, while it was primarily related with the WP pattern in the latter half of this century. This tendency of the change in correlation coefficients between the SOI and the SLP—principal components is also found in the correlation coefficients between the CTI and SLP—principal components. The preferable relation between ENSO and the WP pattern in the latter period was also supported by Tanimoto, Iwasaka and Hanawa (1997). These interdecadal modulations in the teleconnections between ENSO and mid-latitude circulation patterns do not exhibit consistent changes with the strong or weak Aleutian Low.

Variations between ENSO and the mid-latitude circulation might be influenced by interdecadal changes in the intensity of ENSO. The interannual variability of the SOI and Nino 3 SST are known to be strong from 1880 to 1920 and after 1960 (Trenberth, 1990; Torrence & Compo, 1998). Thus, changing ENSO amplitudes do not have a unique relation to the changing correlations between indices for ENSO and the PNA/WP circulation patterns.

Tropical climate variations other than ENSO might influence the interdecadal modulation of the atmospheric circulation in the mid-latitudes. Recently, Kawamura (1998) proposed that tropical SST forcing caused the increased interannual variance of the summer air-temperature observed in Japan from 1977 to 1993 compared with that in the period from 1963 to 1976. They proposed that the increased interannual amplitude in the summertime zonal SST gradient to the east of the Philippine Sea

Table 1
Correlation coefficients between high-pass filtered Southern Oscillation Index (SOI) and EOFs of the 500 hPa height or SLP, and correlation coefficients between high-pass filtered Cold Tongue Index (CTI) and EOFs of SLP

	1899–1924	1925–47	1948–76	1977–94/92
SOI vs. EOF 1-Z500	–	–	0.186	0.597*
SOI vs. EOF 2-Z500	–	–	− 0.504*	− 0.577*
SOI vs. EOF 1-SLP	0.400*	0.337	0.128	0.562*
SOI vs. EOF 2-SLP	− 0.184	− 0.185	− 0.436*	− 0.614*
CTI vs. EOF 1-SLP	− 0.557*	− 0.554*	− 0.203	− 0.547*
CTI vs. EOF 2-SLP	0.359	0.233	0.544*	0.669*

The last year of the fourth period (rightmost column) is 1994 for the upper four rows, and is 1992 for the lower two rows.
Asterisks indicate the correlation coefficient is significant at 95% confidence limit, assuming the data in each year is independent.

caused enhanced interannual variability in geopotential height, which is responsible for the increased interannual variance of the Japanese summer air-temperature. Although similar mechanisms might play a role for the interdecadal modulation of the atmosphere and ocean variability changes in the wintertime North Pacific, further assessments are necessary to evaluate this possibility.

4. Summary and discussion

Aspects of interdecadal modulations of interannual atmospheric and oceanic variability are examined over the North Pacific. The North Pacific Index, an indicator for the strength of Aleutian Low, exhibits relatively high interannual variance from about 1925 to 1945 and in the 1980s, time periods that roughly correspond to regimes of an intensified Aleutian Low associated with a previously identified 50–70 year oscillation in Pacific climate. Supporting evidence for an interdecadal modulation of interannual atmospheric variability is found in an analysis of the temporal coefficient of the first Empirical Orthogonal Function (EOF) of the SLP field over the North Pacific. The second EOF, which is associated with the North Pacific Oscillation, exhibits decreasing interannual variance around 1970 on interdecadal time scales. The expansion coefficients for the first and second eigenvectors of wintertime (December–February) Pacific sector 500 hPa heights exhibit similar interdecadal modulation of interannual variability as that found with the expansion coefficients for the first two eigenvectors of the wintertime SLP field, respectively.

As identified in many previous studies, the leading 500 hPa eigenvector is the Pacific/North American (PNA) teleconnection pattern, while the second eigenvector corresponds to the Western Pacific (WP) pattern. Changes of the interannual variance of the atmospheric circulation are also evident in the interannual variance of North Pacific zonal and meridional wind stress; the variance in the 1977–1994 zonal wind stress increased in the central North Pacific and decreased in the zonal and meridional stress components in the Sea of Okhotsk and Bering Sea.

A basin-scale presence of an interdecadal modulation of interannual variability in Pacific SST and the Pacific sector atmosphere is examined using Singular Value Decomposition (SVD). The leading singular vector pair recovers the salient features of the atmospheric PNA pattern. The temporal coefficients of the first singular vector pair of springtime SST and wintertime 500 hPa height exhibit relatively large interannual variability in the 1970s and 1980s, and relatively weak interannual variability in the period from the 1940s to the 1960s. The temporal coefficient of the second singular vector pair, which is related with the atmospheric WP pattern, exhibited weaker interannual variability in the 1970s. These results indicate that interdecadal modulations of interannual variability over the North Pacific are expressed as variations in the preferred spatial patterns of atmospheric and oceanic variability.

Our examination of coastal SST from each side of the north Pacific basin supports the regime-dependent changes in ocean–atmosphere interactions. The first seasonally combined EOF along the US/Canada coast is strongly related to the PNA pattern for the 1977–1994 period of record, but not for the 1948–1976 period. PNA varia-

bility also likely influences the spring Enoshima SST, which well represents the first EOF mode of the coastal Japanese SST data.

Teleconnection between the mid-latitude North Pacific and tropics exhibit multidecadal modulation, though unique regime dependent changes have not been found. The PNA (WP) pattern is primarily associated with ENSO in the first (last) half of the present century. Correlations between the PNA pattern and indices for ENSO are remarkably weak from the late 1940s to 1970s. Further assessments are necessary to understand the mechanisms causing the low-frequency modulation of interannual time scale teleconnections between the mid-latitudes and tropics.

Bitz and Battisti (1999) find evidence for interdecadal modulations in North Pacific storminess (variance in the 2–7 day period band). The emerging picture of North Pacific climate is one with variability at a range of shorter time scales influenced by that at lower frequencies. Eras with an especially intense Aleutian Low appear to favor enhanced interannual variance in the North Pacific and enhanced (reduced) synoptic scale variance on the southern (northern and northeastern) flanks of the Aleutian Low. Conversely, interdecadal regimes characterized by a relatively weak Aleutian Low are found to also experience relatively weak interannual and intraseasonal variability in the open waters of the North Pacific sector, but enhanced synoptic scale variability over the coastal waters of Alaska.

Interactions between climate variations on different timescales are necessary to be investigated further in future. The influences of the variation of the longer timescale on the shorter timescale variability is examined in the present paper and also by Bitz and Battisti (1999). Such influence might be viewed as responses of perturbation fields to the changes of basic fields on longer timescale. Another important scenario for interactions between different timescales is associated with a stronger nonlinearity in the climate system. For example, Minobe (1999) proposed that the climatic regime shifts over the North Pacific are arose from the phase-locking between the pentadecadal and bidecadal (with a possible period of about 17 year) variations with a relative period of three.

A growing body of research has documented coherence between interdecadal fluctuations in North Pacific climate and marine ecosystems (i.e. Kodama et al., 1995; Mantua et al., 1997; McGowan et al., 1998; Yasuda, Sugusaki, Watanabe, Minobe & Oozeki, 1999). However, the biophysical linkages remain largely unknown. Whether marine ecosystems are more sensitive to changes in the mean climate (first moment) or to interdecadal modulations in interannual and/or even higher frequency variability (second moment) remains unknown.

The interdecadal modulation of the interannaul variability of the Aleutian Low might play an important role not only for marine ecosystems, but also for the physical parameters that play important roles in climate variability. One such parameter is the temperature of upper ocean water masses formed in the central North Pacific. Surface layer temperatures are observed to change depending on the strength of the Aleutian Low (Watanabe & Mizuno, 1994; Deser, Alexander & Timlin, 1996; Schneider, Miller, Alexander & Deser, 1999). Gu and Philander (1997) hypothesized that the thermal properties of mid-latitude water masses play a key role in a delayed negative-feedback oscillator which gives rise to interdecadal variability in North

Pacific climate. Deser et al. (1996) showed that even in the period of a strong mean Aleutian Low (post-1977), long-lived thermal anomalies that persisted in the subsurface ocean were only formed during severe winters. Thus, for periods having a relatively strong (mean-state) Aleutian Low, relatively strong interannual variability is expected to result in more frequent and consequently more climatically significant subsurface thermal anomalies. In summary, changes in the variance rather than changes in the mean strength of the Aleutian Low may play the most critical role in these ocean–atmosphere interactions.

We would like to point out the value of long-term coastal data. As shown in the present paper, the use of long-term coastal data provides us with valuable retrospective information about oceanographic variability prior to World War II. The data from Canada and the United States is carefully collected and made easily available via the World Wide Web. Japanese data, however, are not regularly archived at a data center, and therefore the use of this important data is quite difficult for most researchers. Based on the importance of the long-term SST data, we hope that collection and accessibility of the Japanese long-term SST data will be continued and improved.

5. Acknowledgements

We thank T. P. Mitchell, I. Yasuda, and K. Hanawa for valuable discussions, N. Schneider for sharing his unpublished research results, J. Kodama and S. Ito for Japanese coastal SST data. We also appreciate the comments of D. R. Cayan and H. J. Freeland, who read the original manuscript. Some figures are produced with the GrADS developed by B. Doty. S. Minobe was supported by grants from the Japanese Ministry of Education, Culture and Science. N. Mantua was funded through the NOAA Office of Global Programs project titled ‘An integrated assessment of the dynamics of climate variability, impacts, and policy response strategies’. This publication is funded in part by the Joint Institute for the Study of the Atmosphere and Oceans (JISAO) under NOAA Cooperative Agreement No. NA67RJ0155, Contribution No. 578. The views expressed herein are those of the authors and do not necessarily reflect the views of NOAA or any of its subagencies.

6. References

Bitz, C. C., & Battisti, D. S. (1999). Inter-annual to decadal variability in climate and glacier mass balance in Washington, Western Canada, and Alaska. *Journal of Climate*, in press.

Bottomley, M., Folland, C. K., Hsiung, J., Newell, R. E., & Parker, D. E. (1990). Global ocean surface temperature atlas (GOSTA). (20 + iv pp and 313 plates). Bracknell: UK Meteorological Office.

da Silva, A. M., Young, C. C., & Levitus, S. (1994a). Atlas of surface marine data 1994, Vol. 3: Anomalies of heat and momentum fluxes. NOAA Atlas NESDIS 8 (413 pp.). Washington, DC: US Department of Commerce, National Oceanic and Atmospheric Administration.

da Silva, A. M., Young, C. C., & Levitus, S. (1994b). Atlas of surface marine data 1994, Vol. 2: Anomalies of directly observed quantities. NOAA Atlas NESDIS 7 (416 pp.). Washington, DC: US Department of Commerce, National Oceanic and Atmospheric Administration.

Deser, C., & Wallace, J. M. (1990). Large-scale atmospheric circulation features of warm and cold episodes in the tropical Pacific. *Journal of Climate*, *3*, 1254–1281.

Deser, C., Alexander, A., & Timlin, M. S. (1996). Latent and sensible heat flux anomalies over the upper-ocean thermal variations in the North Pacific during 1970-1991. *Journal of Climate*, *9*, 1840–1855.

Farge, M. (1992). Wavelet transforms and their applications to turbulence. *Annual Review of Fluid Mechanics*, *24*, 395–457.

Graham, N. E. (1994). Decadal scale variability in the 1970s and 1980s: observations and model results. *Climate Dynamics*, *10*, 135–162.

Gu, D. F., & Philander, S. G. H. (1995). Secular changes of annual and interannual variability in the tropics during the past century. *Journal of Climate*, *8*, 864–876.

Gu, D. F., & Philander, S. G. H. (1997). Interdecadal climate fluctuations that depend on exchanges between the tropics and extratropics. *Science*, *275*, 805–807.

Hanawa, K. (1997). Characteristics of long-term variations of summertime temperature in northeastern Japan (in Japanese). *Kishou Kenkyuu Note*, *189*, 192–198.

Hare, S. R., & Francis, R. C. (1995). Climate change and salmon production in the Northeast Pacific Ocean. In R. J. Beamish (Ed.), Ocean climate and northern fish populations (pp. 357–372). Canadian Special Publication of Fisheries and Aquatic Sciences.

Kawamura, R. (1998). Recent Extraordinary cool and hot summers in east Asia simulated by an ensemble climate experiment. *Journal of the Meteorological Society of Japan*, *76*, 597–617.

Kodaman, J., Nagashima, H., & Izumi, Y. (1995). Long-term variations in the 'mongoku herring', clupea pallasi valenciennes resources in relation to the ocean environments in the waters off sanrikua and Joban (in Japanese). *Bulletin of Miyagi Prefecture Fishery Research Division Center*, *14*, 17–36.

Koide, H., & Kodera, K. (1997). Characteristics of the recent long-term wintertime variability in the atmosphere and oceans (in Japanese). *Tenki*, *44*, 3–17.

Lau, K. -M., & Weng, H. (1995). Climate signal detection using wavelet transform: how to make a time series sing. *Bulletin of the American Meteorological Society*, *76*, 2391–2402.

Mantua, N. J., Hare, S. R., Zhang, Y., Wallace, J. M., & Francis, R. C. (1997). A Pacific interdecadal climate oscillation with impacts on salmon production. *Bulletin of American Meteorological Society*, *76*, 1069–1079.

McGowan, J. A., Cayan, D. R., & Dorman, L. M. (1998). Climate–ocean variability and ecosystem response in the Northeast Pacific. *Science*, *281*, 210–217.

Minobe, S. (1997). A 50–70 year climatic oscillation over the North Pacific and North America. *Geophysical Research Letters*, *24*, 683–686.

Minobe, S. (1999). Resonance in bidecadal and pentadecadal climate oscillations over the North Pacific: role in climate regime shifts. *Geophysical Research Letters*, *26*, 855–858.

Nakamura, H., Lin, G., & Yamagata, T. (1997). Decadal climate variability in the North Pacific during the recent decades. *Bulletin of American Meteorological Society*, *98*, 2215–2225.

Namias, J., Yuan, X., & Cayan, D. R. (1988). Persistence of North Pacific sea surface temperature and atmospheric flow patterns. *Journal of Climate*, *1*, 682–703.

Nitta, T., & Yamada, S. (1989). Recent warming of tropical sea surface temperature and its relationship to the Northern Hemisphere circulation. *Journal of Meteorological Society of Japan*, *67*, 375–383.

Rogers, J. C. (1981). The North-Pacific oscillation. *Journal of Climatology*, *1*, 39–52.

Schneider, N.A., Alexander, M.A., Miller, A.J., & Deser, C. (1999). Subduction of decadal North Pacific temperature anomalies: observations and dynamics. *Journal of Physical Oceanography*, *29*, 1056–1090.

Sekine, Y. (1988). Anomalous southward intrusion of the Oyashio east of Japan 1. Influence of the seasonal and interannual variations in the wind stress over the North Pacific. *Journal of Geophysical Research*, *93*, 2247–2255.

Tanimoto, Y., Iwasaka, N., Hanawa, K., & Toba, Y. (1993). Characteristic variation of sea surface temprature with multiple time scale in the North Pacific. *Journal of Climate*, *6*, 1153–1160.

Tanimoto, Y., Iwasaka, N., & Hanawa, K. (1997). Relationships between sea surface temperature, the atmospheric circulation and air–sea fluxes on multiple time scales. *Journal of Meteorological Society of Japan*, *75*, 831–849.

Torrence, C., & Compo, G. P. (1998). A practical guide to wavelet analysis. *Bulletin of the American Meteorological Society*, *79*, 61–78.

Trenberth, K. E. (1990). Recent observed interdecadal climate changes in the Northern Hemisphere. *Bulletin of American Meteorological Society*, *71*, 988–993.

Trenberth, K. E., & Paolino, D. A. (1980). The Northern Hemisphere sea-level pressure data set: trends, errors, and discontinuities. *Monthly Weather Review*, *108*, 855–872.

Trenberth, K. E., & Hurrel, J. W. (1994). Decadal atmosphere–ocean variations in the Pacific. *Climate Dynamics*, *9*, 303–319.

Walker, G. T., & Bliss, E. W. (1932). World weather V. *Memoirs of the Royal Meteorological Society*, *4*, 53–84.

Wallace, J. M., & Gutzler, D. S. (1981). Teleconnections in the geopotential height field during the Northern Hemisphere winter. *Monthly Weather Review*, *109*, 784–812.

Wallace, J. M., Smith, C., & Bretherton, C. S. (1992). Singular value decomposition of wintertime sea surface temperature and 500-mb height anomalies. *Journal of Climate*, *5*, 561–577.

Watanabe, T., & Mizuno, K. (1994). Decadal changes in the thermal structure of the North Pacific. *International WOCE Newsletter*, *15*, 10–13.

Weng, H., & Lau, K. -M. (1994). Wavelets, period doubling, and time-frequency localization with application to organization of convection over the tropical western Pacific. *Journal of Atmospheric Science*, *51*, 2523–2541.

Yasuda, I., Sugusaki, H., Watanabe, Y., Minobe, S., & Oozeki, Y. (1999). Inter-decadal variations in Japanese sardine and ocean/climate. *Fisheries Oceanography*, *8*, 18–24.

Zhang, Y., Wallace, J. M., & Battisti, D. S. (1997). ENSO-like interdecadal variability: 1900–1993. *Journal of Climate*, *10*, 1004–1020.